Measurement of coherent tunneling between InGaAs quantum wells and InAs quantum dots using photoluminescence spectroscopy

Yu. I. Mazur,* V. G. Dorogan, D. Guzun, E. Marega, Jr.,† and G. J. Salamo
Department of Physics, University of Arkansas, 226 Physics Building, Fayetteville, Arkansas 72701, USA

G. G. Tarasov
Institute of Semiconductor Physics, National Academy of Sciences of Ukraine, pr. Nauki 45, Kiev-03028, Ukraine

A. O. Govorov
Department of Physics and Astronomy, Ohio University, Athens, Ohio 45701, USA

P. Vasa and C. Lienau
Institut für Physik, Carl von Ossietzky Universität, 26111 Oldenburg, Germany
(Received 31 July 2010; published 8 October 2010)

We present a spectroscopic manifestation of the intermediate coherent tunneling regime between a quantum-dot (QD) and a quantum-well (QW) layer. We observe a nontrivial dependence of the resonant QD photoluminescence excitation (PLE) signal as a function of dot-well barrier thickness. For thick barriers and resonant QW excitation, the photogenerated QD carrier density increases exponentially with increasing coupling strength. For separations of a few nanometers only, however, we observe an anomalous decrease in the PLE signal. This behavior is defined by subpicosecond resonant coherent tunneling dynamics between the QW and QD. Our results shed light on the intermediate coherent tunneling regime of relevance in a variety of functional nanostructures such as charge or spin injectors or photovoltaic devices.

DOI: 10.1103/PhysRevB.82.155413 PACS number(s): 78.67.Hc, 73.40.Gk, 78.55.Cr, 78.67.De

The ultrafast optically induced injection of electrical charges (electrons and/or holes) is of fundamental importance for the function of a broad variety of nanostructures, ranging from biological photoreceptors, such as rhodopsin in the retina[1] and the light harvesting complex in photosynthetic membranes,[2] to artificial nanostructures, such as quantum cascade lasers,[3] high speed photodiodes, and photovoltaic devices.[4,5] In most of these structures, electron injection is thought to be an incoherent relaxation phenomenon, resulting in a rapid transfer of charges between a donor and an acceptor state.[6] Coherent phenomena, such as Rabi oscillations between the donor and acceptor state, resulting in the hybridization of quantum states, are believed to be of relevance only for a limited class of carefully designed nanostructures, such as, e.g., two individual quantum dots (QDs) tuned into resonance by means of external electric fields, which has recently attracted considerable interest as an example of a tunable system in a strong-coupling regime.[7,8] This has enabled detailed studies of systems where the coupling strength is larger than both the dephasing rate of the individual resonances and the detuning between the coupled states. Here, we explore coherent tunneling phenomena in a prototypical two-dimensional (2D)-zero-dimensional (0D) hybrid tunnel injection structure of immediate relevance for device applications. In this structure the carrier injector, a quasi-2D quantum well (QW) is spatially separated by a tunneling barrier from a (0D) QD layer. Through this tunneling barrier, cold carriers (electrons and/or holes) transfer from 2D QW states into localized QD states. This results, e.g., in reduced carrier/phonon heating and increased differential gain in QD lasers.[9,10] In such structures coherent tunneling effects have remained unexplored. Existing theoretical and experimental work has mainly focused on the appearance of asymmetric optical line shapes.[11–14] These line shapes are thought to arise, in analogy to the well-known Fano resonance in atomic physics,[15] from the interference between emission from weakly electronically coupled localized 0D and 2D continuum states. Such 2D-0D hybrid structures should be well suited for exploring coherent tunneling phenomena since the coupling strength and thus the degree of quantum state hybridization can be controlled over a wide range by varying the thickness and/or composition of the tunneling barrier.

Here, we present the systematic study of coherent tunneling between quantum wells and quantum dots in hybrid 2D-0D nanostructures. Photoluminescence excitation (PLE) spectra for resonant QW excitation reveal an unexpected, nonmonotonic dependence of the optically generated QD carrier density on the dot-well barrier thickness. We demonstrate that the decrease in QD carrier density observed for small barrier thicknesses is an inherent signature of the intermediate coherent tunneling regime[16] in these hybrid structures, in which the coupling strength is of the same order as the optical dephasing rate. These conclusions, drawn from quasistationary PL and PLE experiments are corroborated by direct time-resolved studies of the tunneling dynamics.

A series of InAs QDs/InGaAs QW hybrid nanostructures, schematically depicted in Fig. 1(a) with controlled tunneling barriers were grown by molecular-beam epitaxy on semi-insulating GaAs (001) substrates. Subsequent to the growth of an 0.3-μm-thick GaAs buffer layer deposited at 580 °C to smoothen the surface, the temperature was lowered to 530 °C. After growth of a 15-nm-thick $In_{0.13}Ga_{0.87}As$ QW and a 30 s interruption, a GaAs barrier layer was deposited

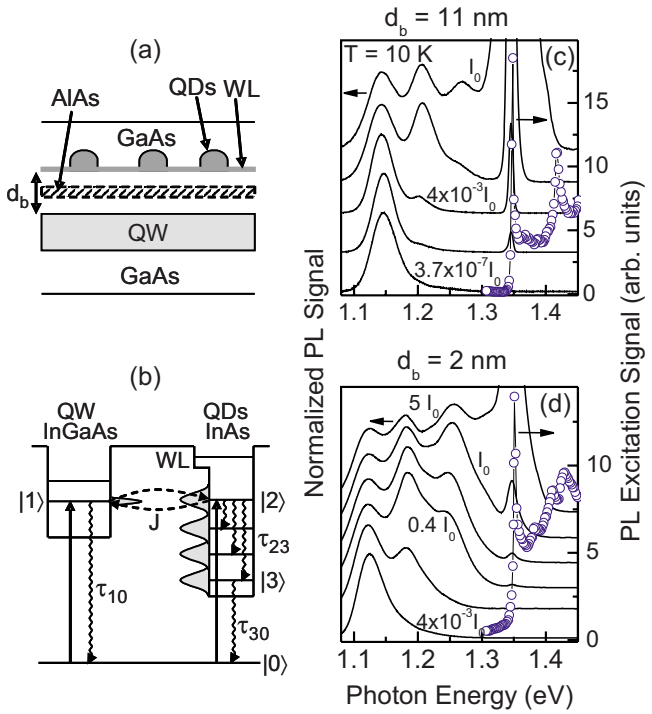

FIG. 1. (Color online) (a) Schematic presentation of the hybrid $In_{0.13}Ga_{0.87}As$ QW/InAs QD structure; (b) energy scheme of the structure and transitions under investigation. Relaxation processes are shown as wavy arrows; optical transitions are depicted by straight arrows. The QW and QD density of states are shown by shadowed areas; PL (solid lines) and PLE spectra (open circles) measured in the hybrid InAs QDs/$In_{0.13}Ga_{0.87}As$ QW nanostructures with (c) d_b=11 nm and (d) d_b=2 nm at different excitation intensities at T=10 K. The spectra are shifted vertically for clarity, I_0=1000 W/cm^2.

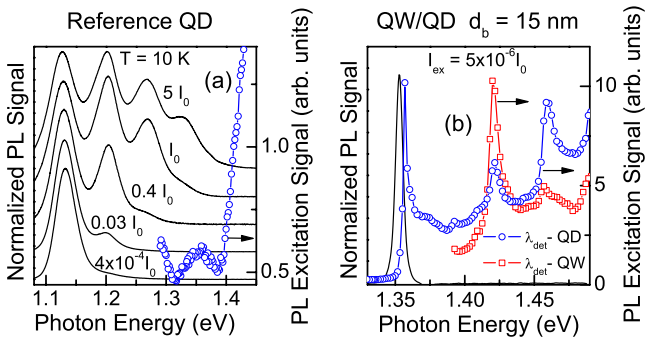

FIG. 2. (Color online) (a) Low-temperature (T=10 K) PL and PLE spectra measured at different excitation intensities in a reference sample containing only an InAs QD layer. The spectra are shifted vertically for clarity. I_0=1000 W/cm^2. (b) PLE spectra measured in the hybrid $In_{0.13}Ga_{0.87}As$ QW/InAs QD structure with d_b=15 nm for an excitation intensity of $1.5\times10^{-6}I_0$. The spectra are recorded detecting the QD ground-state emission (E_{det} =1.148 eV, open circles) and QW exciton emission (E_{det} =1.348 eV, open squares), respectively. The QW PL spectrum (solid line) has been recorded at an excitation intensity of $5\times10^{-6}I_0$.

with a thickness that was varied between 1 and 20 nm within the series of samples. In some samples, a symmetric, 1–4-nm-thick AlAs layer was incorporated inside the GaAs barrier. A 2-monolayer-thick InAs QD film was then deposited onto the GaAs spacer and finally the structures were covered with a 50 nm GaAs cap. Analysis by atomic force microscopy revealed a QD areal density $\sim10^{10}$ cm^{-2} and average QD height of 5 nm. PL measurements were performed with excitation wavelength at λ_{exc}=532 nm at a temperature of 10 K. The laser was focused to a spot size of $\sim$20 μm and the optical excitation power was varied over the range from $\sim(10^{-6}-10^{2})$ mW. For the resonant PL and PLE measurements a tunable Ti:sapphire laser was used. Time-resolved studies of the tunneling dynamics are performed in a noncollinear pump-probe setup. Ultrafast laser pulses with a duration of 220 fs and a center wavelength of 920 nm are generated in a tunable Ti:sapphire laser operating at a repetition rate of 76 MHz. Linear polarized pump and probe pulses with orthogonal polarization and with pulse energies of 30 pJ and 5.5 pJ, respectively, are focused onto the sample to a spot size of 200 μm. The reflected probe laser pulse is spectrally dispersed in an 1/8 m monochromator and detected with a silicon photodiode. The pump-induced change in probe reflectivity $\Delta R(\lambda,\Delta t)=R(\lambda,\Delta t)-R_0(\lambda)$ is recorded as a function of the time delay Δt between the pump and probe lasers. Here, R and R_0 denote the probe laser reflectivity in the presence and absence of a pump laser, respectively.

Figure 1 shows PL spectra measured under different excitation intensities in InAs QD/$In_{0.13}Ga_{0.87}As$ QW samples with GaAs barriers with thickness of (c) d_b=11 nm and (d) d_b=2 nm. For all investigated samples, the low excitation intensity ($I_{exc}\leq4\times10^{-4}I_0$ and I_0=1000 W/cm^2) revealed a PL spectrum with a single, approximately Gaussian-shaped PL band, with a maximum at an emission energy of E_{max} =1.145±0.010 eV and a full width at half maximum (FWHM) of $\sim$38±5 meV. This PL band is ascribed to ground-state emission from an inhomogeneously broadened ensemble of QDs, slightly differing in size, shape, and/or composition. With increasing I_{exc} additional PL bands emerge at higher energies which are assigned to dipole-allowed interband transitions from excited QD states. It is generally believed that an increasing I_{exc} results in state filling of low-energy QD states, as indicated by the saturation of the PL emission from these states and an increasing PL emission from higher-lying states.

In a reference QD sample, we observe emission with increasing I_{exc} from all states up to the third excited state at $\sim$1.340 eV [Fig. 2(a)]. The energy spacing between adjacent PL bands is found to be $\sim$66 meV. In the hybrid QW-QD samples, we observe—in this energy region—emission from both the third excited QD state and the QW, in agreement with finding a low-temperature PL peak at E^X $\sim$1.35 eV (FWHM 8 meV) in a reference $In_{0.13}Ga_{0.87}As$ QW sample. QD PLE spectra recorded in the energy range between 1.3 and 1.5 eV [Fig. 2(a)] display a distinct absorption resonance due to the third excited QD state with a FWHM of 35 meV at $E^3_{exc}\sim$1.350 eV, slightly Stokes shifted with respect to the corresponding PL band. The strong increase in PLE signal around 1.4 eV defines the onset of absorption due to the wetting layer (WL). The PLE spectra for the hybrid structure with a thick barrier layer [Fig.

1(c), open circles, and Fig. 2(b)] show two pronounced resonances at 1.35 and 1.42 eV, reflecting the two lowest energy exciton subbands of the QW. The higher energy peak at 1.455 eV represents the WL absorption resonance. In the hybrid structures with a thin barrier layer [Fig. 1(d), open circles], the shape of the PLE spectrum changes. A low-energy tail develops below the lowest exciton resonance and the individual resonances become slightly asymmetric. In our hybrid structure, a discrete resonance (the spectrally narrow QW exciton) is coupled to a spectrally broad resonance (the third excited QD state). In such a situation,[13–15] the interference between the QW and QD emission gives rise to an asymmetric line shape as first discussed by Fano.[15] In general, a detailed line-shape analysis can provide important insight into the quantum-mechanical coupling between the two states. In the present case, however, a meaningful line-shape analysis is complicated due to the predominant inhomogeneous broadening of both the QD and QW emission. Nevertheless, this change in line shape in Fig. 1(d) may be taken as a first signature of the coupling between QW and QD states.

Based on these experiments, we propose the schematic energy structure of the hybrid QW-QD structures depicted in Fig. 1(b). The energy structure is presented in an excitonic basis and has been verified by numerical simulations. The PL and PLE data clearly support the close resonance between the lowest energy $1s$ QW exciton state ($|1\rangle$) and the third excited QD state ($|2\rangle$). This makes these 2D-0D hybrid structures particularly attractive to explore coherent tunneling effects.

To this end we first study the ratio between the QW (at 1.33 eV) and QD PL intensity (at 1.145 eV), taken from spectra similar to those in Figs. 1(c) and 1(d), as a function of d_b for two different excitation intensities of 0.15 $\mathrm{W/cm^2}$ (open circles) and 50 $\mathrm{W/cm^2}$ (closed circles), respectively [Fig. 3(a)]. The data are also plotted as a function of the carrier transmission through the barrier $T(E) \propto \exp\{-\int_0^{d_b}[V(x)-E]^{1/2}dx\}$, where $V(x)$ is the barrier band gap and $E=E^X$. With decreasing d_b, i.e., increasing transmission, we find a clear increase in QD emission. This shows that an increasing number of electron-hole pairs are transferred from the QW into the QDs. The data also show that for small d_b state filling of QW levels becomes more prominent for higher excitation intensities (open circles) so that the relative QD PL increases with increasing excitation intensity.

The carrier transfer between QW and QDs is then more directly probed for resonant QW excitation. In all samples, PLE spectra were recorded at a fixed excitation intensity of $1.5\times10^{-6}I_0$. The ground-state QD PL was monitored while tuning the excitation wavelength around the QW exciton resonance. The excitation intensity was sufficiently low to avoid state-filling effects. The maximum QD PL intensity (at 1.145 eV) observed for resonant QW excitation was measured and is plotted in Fig. 3(a) (open triangles) as a function of d_b and T (in relative units).

For large d_b, the QD PL is weak since tunneling between QW and QD excited states is efficiently suppressed. With decreasing d_b the QD PL first increases quickly by two orders of magnitude, then reaches a maximum near $d_b=8$ nm until it begins to even decrease for $d_b<3$ nm. This indicates that the tunneling-induced transfer of optical excitations

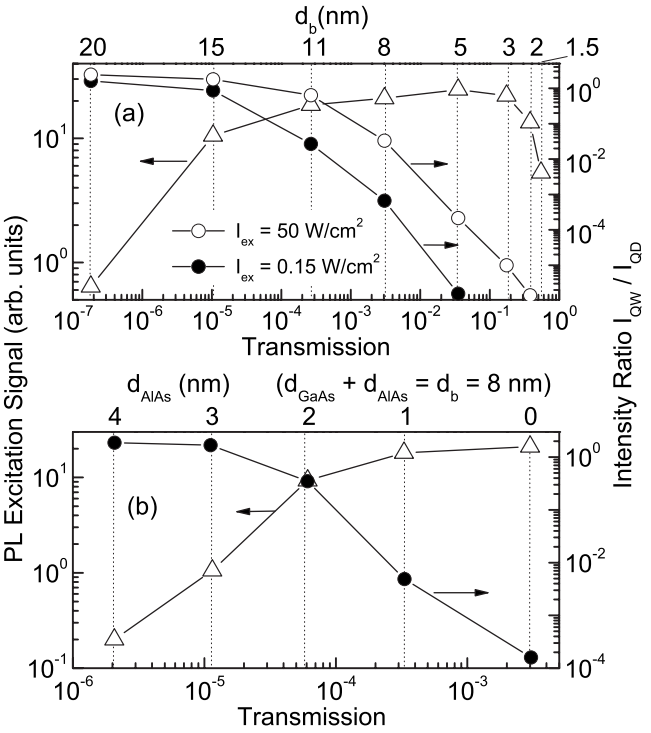

FIG. 3. (a) QD PLE signal under resonant excitation of the QW versus barrier transmission T calculated for the GaAs barrier thicknesses d_b shown in the top abscissa. The ratio of the maximum QW and QD PL intensity is shown for nonresonant excitation ($\lambda_{exc}=532$ nm) at two different excitation intensities of 50 $\mathrm{W/cm^2}$ (open circles) and 0.15 $\mathrm{W/cm^2}$ (closed circles); (b) the same dependencies as in Fig. 3(a) measured for composite GaAs barrier including AlAs layer with different thicknesses.

from the QW to the QD decreases sharply for very thin barriers even though the transmission T continues to increase by almost one order of magnitude. This surprising, and unexpected, behavior will be analyzed in detail below. The data in Fig. 3(b) summarizes similar results for different samples with a total barrier thickness $d_b=8$ nm. In these samples, the tunneling transmission T is varied by three orders of magnitude by incorporating an AlAs layer into the GaAs barrier. An increase in the thickness of the AlAs layer results in a suppression of tunnel coupling and therefore an increase in QW PL and a corresponding decrease in the PLE signal.

To appropriately describe the effects of coherent tunneling dynamics, we model these experiments within the framework of the optical Bloch equations. For simplicity, we consider a four-level system, consisting of a crystal ground state $|0\rangle$, a QW $1s$-exciton state $|1\rangle$, an excited QD state $|2\rangle$, and a QD ground state $|3\rangle$ with energies $\hbar\omega_i$, $i=0,\ldots,3$.

One may certainly question whether it is appropriate to model the QW exciton by a single exciton state, neglecting the quasi-two-dimensional density of QW states. We justify this choice by noting that we did not observe clear signatures of quasi-2D QW character on the carrier transfer between QW and QD. Hence, such a four-level model turned out to be the simplest physical model which can reproduce the salient findings of our work. We also note that optical spectra of the QW in these hybrid structures are predominantly inhomoge-

neously broadened. We therefore expect that the tunneling physics studied here is essentially that of a localized QW state coupled to an excited QD state. Therefore the tunneling dynamics are expected to depend sensitively on the details of the exciton localization in the QW. The simplified four-level scheme outlined above can certainly give only qualitative, ensemble-averaged information. More sophisticated models might be needed once more information about exciton localization in these hybrid structures and its influence on the carrier transfer dynamics is available.

Here, however, the main emphasis lies on describing the surprising decrease in PLE intensity for thin barriers seen in Fig. 3(a) and we will show below that the above simplified model can indeed reproduce these findings. We consider optical excitation of the four-level system with a monochromatic light field of amplitude $E_0(\omega_L)$ and frequency ω_L induces optical QW and QD polarizations ρ_{0i}, $i=1,\ldots,3$, respectively, where ρ_{ij} denote the usual elements of the density matrix. The equations of motion for these polarizations are given as

$$\dot{\rho}_{01} = -i\delta_1\rho_{01} - i\Omega_1(\rho_{11}-\rho_{00}) + iJ\rho_{02} - \gamma_1'\rho_{01},$$

$$\dot{\rho}_{02} = -i\delta_2\rho_{02} - i\Omega_2(\rho_{22}-\rho_{00}) + iJ\rho_{01} - \gamma_2'\rho_{02}. \quad (1)$$

Here, $\delta_i=\omega_L-\omega_i+\omega_0$ denote the detunings, $\Omega_i=d_iE_0(\omega_L)$ the Rabi frequencies with d_i being the relevant transition dipole moments, γ_i' the dephasing rates, and J the tunnel coupling matrix element between states $|1\rangle$ and $|2\rangle$. The tunnel coupling induces Rabi oscillations between the two coupled states and the equation of motion for the relevant coherent polarization is

$$\dot{\rho}_{12} = -i\delta_3\rho_{12} - iJ(\rho_{22}-\rho_{11}) - \gamma_3'\rho_{12} \quad (2)$$

with $\delta_3=\omega_1-\omega_2$. As already well known, the Bloch equations also provide equations of motions for the state populations, specifically

$$\dot{\rho}_{11} = -2\Omega_1\,\mathrm{Im}(\rho_{01}) - 2J\,\mathrm{Im}(\rho_{12}) - \gamma_{10}\rho_{11},$$

$$\dot{\rho}_{22} = -2\Omega_2\,\mathrm{Im}(\rho_{02}) + 2J\,\mathrm{Im}(\rho_{12}) - (\gamma_{23}+\gamma_{20})\rho_{22},$$

$$\dot{\rho}_{33} = \gamma_{23}\rho_{22} - \gamma_{30}\rho_{33}. \quad (3)$$

We assume that the excitation laser is sufficiently detuned from $|3\rangle$ so that we can neglect resonant excitation of the QD ground state. The relaxation rates γ_{i0} describe (radiative) population relaxation to the ground state whereas γ_{23} describes the phonon-mediated population relaxation between the excited QD level and its ground state. To compare with the experimental PLE data shown in Fig. 4(a), we numerically analyze these equations in the quasistationary limit $d\rho_{ij}/dt=0$ as a function of laser frequency ω_L and tunnel coupling strength J. For this analysis it is important that the intradot relaxation rate γ_{23} is by far the fastest of all relaxation rates. In InAs QDs, intradot relaxation rates are short and typically lie in the range of a few picoseconds,[17,18] partly due to the strong electron-phonon coupling in these systems and the resulting short polaron lifetimes.[19] We therefore always assume that $\gamma_{23}\gg\gamma_{10}$, i.e., that the lifetime of excited

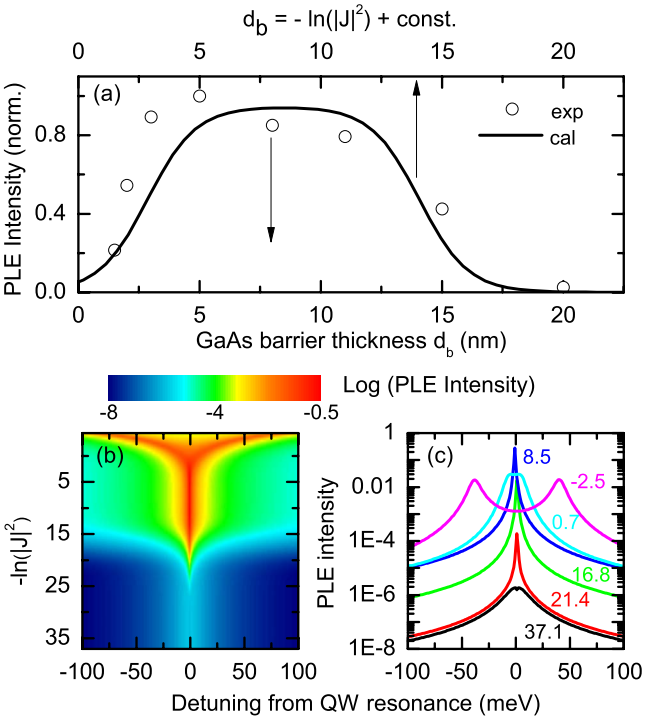

FIG. 4. (Color online) (a) Normalized QD PLE signal under resonant excitation of the QW versus GaAs barrier thickness d_b (bottom abscissa). The results from the Bloch equation model (solid line) are as a function logarithm of the square of the coupling constant $-\ln(|J^2|)$. (b) QD PLE spectra for resonant QW excitation calculated within Bloch equation model as a function of $-\ln(|J^2|)$. (c) Simulated PLE spectra for various values of $-\ln(|J^2|)$.

QD states is much shorter than the QW PL decay time ($\approx$500 ps). For simplicity, we also assume that the levels $|1\rangle$ and $|2\rangle$ are exactly on resonance. Essentially, in this limit, the model simulations satisfactorily describe the observed distance dependence of the experimental PLE intensity [Fig. 4(a)]. We critically checked that the conclusions drawn from these simulations are also valid for finite detunings between both levels. Small detunings are certainly expected in our samples. The PL spectra in Fig. 1, e.g., show a slight gradual redshift of the QD ground-state energy by about 25 meV when changing the barrier from 20 to 2 nm. Similarly, also the QW exciton resonance shifts slightly to the red with decreasing barrier thickness. A careful inspection of PL and PLE spectra allows us to conclude that the ensemble-averaged detuning between $|1\rangle$ and $|2\rangle$ differs by less than 15 meV in all samples of this study. This rather small detuning therefore can certainly not account for the more than fourfold decrease seen in PLE intensity in Fig. 3 for thin barriers. These qualitative statements are fully confirmed by comparing model calculations with and without detuning.

To correlate coupling strength J and barrier thickness d_b we take $T\propto|J|^2$ in the limit of Fermi's golden rule, and hence $d_b=-2\ln(|J|)+c$, where c is the constant. The Bloch equation model clearly reproduces the observed saturation of the PLE intensity and the PLE decrease for small d_b. The physics underlying this behavior becomes transparent by inspecting the J-dependent variation in shape of the PLE spectra [Figs. 4(b) and 4(c)]. For small J ($-\ln|J|^2=37.1$), tunnel cou-

pling is negligible and the PLE spectrum simply reflects the QD excited state absorption spectrum. Here, γ_{10}, taken as 2 ns^{-1}, is sufficiently fast to fully suppress tunneling. With increasing J $(-\ln|J|^2=37.1-8.5)$, tunneling occurs on time scales approaching γ_{10}^{-1} and the number of carriers tunneling into QD states increases exponentially with J. In this weak-coupling limit, the PLE spectrum is simply given as a sum of the QW and QD absorption spectrum. For J corresponding to tunneling on time scales shorter than γ_{10}^{-1} but larger than γ_{23}^{-1}, here taken as 0.3 ps^{-1}, essentially all carriers being optically excited in the QW can tunnel into excited QD states and relax into the QD ground state. Therefore, the PLE intensity saturates while the spectra are still given as a sum of QW and QD spectra. For $J>h\gamma_{23}$ $(-\ln|J|^2=0.7)$, Rabi oscillations between levels $|1\rangle$ and $|2\rangle$ set in, resulting in a broadening of the PLE spectrum from the hybridization of QW and QD excitations. In this intermediate coupling regime J and $h\gamma_{23}$ become comparable, resulting in strongly damped Rabi oscillations and broadened PLE spectra which lead to a decrease in PLE signal for resonant QW excitation. It is this intermediate-coupling regime which is obviously reached in our experiments for samples with $d_b \leq 3$ nm. At even larger coupling strength $(-\ln|J|^2<-1)$, the strong-coupling regime is reached and tunneling-induced hybridization of QW and QD excitations leads to the formation of new, coupled resonances which are energetically split by more than their linewidth as predicted for $J=-2.5$ in Fig. 4(c). Such a splitting of the resonances in the PLE spectra is not observed experimentally and, hence, the strong-coupling regime is likely not reached in our system. We note that the width of the plateau region in Fig. 4(a) depends sensitively on the ratio of γ_{23}/γ_{10} and its existence demonstrates indeed $\gamma_{23} \gg \gamma_{10}$.

Our PLE experiments make clear predictions about the tunneling dynamics in this coupled system. The decrease in PLE is only seen for $J>h\gamma_{23}$, indicating tunneling dynamics on a time scale of at most a few picoseconds, for the thinnest barriers even on a subpicosecond time scale. Such fast tunneling dynamics are apparently at odds with recent time-resolved measurements on similar systems done with nonresonant excitation.[20] The tunneling times deduced from both the QW PL decay and the QD PL rise have been found to be in strong contradiction with the predictions of WKB theory of quantum-mechanical tunneling through barrier, which gives a tunneling time of more than 100 ps for samples with 5 nm barriers. Abrupt reduction in the tunneling time for samples less than 5 nm barriers has been attributed to the formation of nanobridges across the barrier.[20] Obviously, this is not our case, and the physical nature of the observed reduction in our well-dot samples must be established. We therefore performed additional pump-probe experiments to study the tunneling dynamics in our samples in a more direct way. Orthogonally polarized pump and probe pulses with a duration of 200 fs and spectral bandwidth of 10 nm are centered at 920 nm, i.e., around the QW exciton resonance E^X. Spectrally resolved differential reflectivity spectra $\Delta R(\lambda,\Delta t)/R_0(\lambda)=[R(\lambda,\Delta t)-R_0(\lambda)]/R_0$ recorded in such a setup for a hybrid QW/QD sample with a barrier thickness of 5 nm are shown in Fig. 5(a). The spectra display a pronounced transient optical nonlinearity around the QW exciton resonance. For negative delta times,

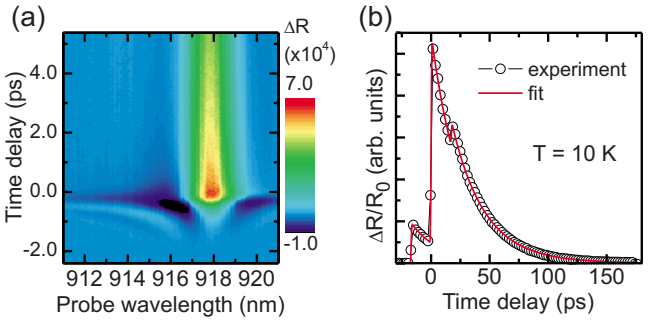

FIG. 5. (Color online) (a) Time-resolved femtosecond differential reflectivity spectra $\Delta R(\lambda,\Delta t)/R_0(\lambda)$ of a hybrid QW/QD sample with a barrier thickness of 5 nm. Orthogonally pump and probe pulses with a wavelength of 920 nm are centered at the QW exciton resonance. The ΔR spectra show (i) at positive delay, $\Delta t>0$, a pump-induced bleaching of the QW exciton resonance persisting for 25 ps, i.e., the QW lifetime and (ii) at negative delay, $\Delta t<0$, spectral oscillations reflecting the perturbed free induction decay of the excitonic QW polarization. (b) Time dynamics of the differential reflectivity $\Delta R(\lambda=hc/E^X,\Delta t)$ probed at the QW exciton resonance (open circles). A single exponential decay of ΔR with a lifetime $\tau_X=25$ ps, reflecting the QW exciton lifetime, is observed. The weak prepulse and after pulse result from reflections of the pump and probe pulses at the rear side of the 0.65-mm-thick sample substrate. The solid line represents a fit to the data using a single-exponential decay.

$\Delta t<0$, pronounced spectral oscillations are observed, reflecting the perturbed free-induction decay of the QW exciton polarization.[21–23] Here, the weak probe pulses are first to interact with the sample and induce a coherent polarization of the inhomogeneously broadened ensemble of QW excitons. This polarization decays with a lifetime T_2, the inverse of the inhomogeneously broadened linewidth of the exciton resonance in the QW PLE spectrum. The optical excitation induced by the strong pump laser may now perturb this free-induction decay and results in a pump-induced reduction in the polarization decay time T_2. This so-called excitation-induced dephasing has been analyzed before both experimentally and theoretically[21–23] and gives rise to the spectral oscillations in $\Delta R(\lambda,\Delta t<0)$. Their analysis therefore provides information about the polarization dynamics of the QW excitons, which, however, is beyond the scope of this work. Here, we are specifically interested in the dynamics of the optical nonlinearity at positive delay times. In this case, the dominant contribution to the optical nonlinearity is the bleaching of the excitonic QW absorption induced by the interaction of the strong pump laser with the sample. This conclusion is supported by finding for $\Delta t>0$ a spectral line shape which is independent on Δt and essentially matches that of the QW PLE spectrum shown in Fig. 2(b). The time dynamics of the differential reflectivity $\Delta R(\lambda=hc/E^X,\Delta t)$ probed at the QW exciton resonance [Fig. 5(b), open circles] therefore allow us deduce the QW exciton lifetime directly. Essentially, the data show a single exponential decay of ΔR with a lifetime $\tau_X=25$ ps. Weak prepulse and after pulse resulting from reflections of the pump and probe pulses at the rear side of the 0.7-mm-thick sample substrate give rise to slight additional peaks in ΔR at delay times of ± 15 ps.

The solid line in Fig. 5(b) represents a single-exponential fit with $\tau_X = 25$ ps to the data. We therefore deduce a QW exciton lifetime of only 25 ps for the hybrid sample with a 5 nm barrier. This lifetime is much shorter than the typical QW exciton lifetimes [24] those of about 500 ps found in reference measurements on a bare QW sample and on a sample with a 20-nm-thick barrier. We therefore conclude that this short lifetime is governed by tunneling-induced decay of the QW exciton population. Such a tunneling time of only 25 ps is in good agreement with the conclusions drawn from the quasistationary PL and PLE experiments. Due to exponential barrier thickness dependence of the tunneling time, the 25 ps lifetime for a 5 nm barrier indicates tunneling times of similar or less than 1 ps for the samples with the thinnest barrier. This strongly supports our assertion that the intermediate coherent tunneling regime is reached in our samples and provides independent evidence that the observed decrease in PLE intensity indeed reflects the onset of Rabi oscillations between QW $|1\rangle$ and excited QD $|2\rangle$ states. More refined pump-probe measurements aimed at probing the effects of these Rabi oscillations on the optical nonlinearities of tunnel-coupled QW/QD hybrid structures in real time are currently underway in our laboratory.

Such a fast tunneling time found for a sample with a rather thick 5 nm barrier allows us comment about the microscopic nature of the tunneling process. The quasistationary PL and PLE experiments cannot distinguish between excitonic and/or single particle tunneling and we have tacitly assumed that the physics is governed by exciton tunneling. Based on the fast 25 ps tunneling time, however, it seems rather straightforward to rule out hole tunneling. Due to the higher mass of the holes, hole tunneling times are orders of magnitude slower than electron tunneling times.[25,26] Therefore hole tunneling is expected to be essentially absent on a time scale of a few picoseconds or even below, i.e., the tunneling time scale predicted by the model calculations and confirmed by the pump-probe data. We therefore assume the tunneling dynamics studied here are mainly governed by electron tunneling, whereas hole tunneling is too slow to contribute significantly. Again, more refined time-resolved studies, distinguishing between nonequilibrium excitonic and single-particle excitations may help in resolving these issues.[27]

In summary, we have presented a systematic study of the intermediate-coupling regime in tunnel-coupled quantum-well-quantum-dot heterostructures. A nontrivial barrier-thickness dependence of PL and PLE is observed which is consistently explained in terms of the tunneling between barrier QW and excited QD states. Our data do give no evidence that other possible coupling mechanisms, e.g., Föerster coupling, contribute significantly to the carrier transfer between QW and QD.

Most interestingly, our results indicate that the hybridization between an excited QD state and localized QW states leads to an anomalous barrier-thickness dependence of the QD PLE signal under resonant QW excitation, governed by surprisingly fast picoseconds to subpicosecond resonant tunneling dynamics for structures with thin barriers. Such tunneling processes are of key importance for the functionality of various nanodevices including, e.g., charge or spin injectors or organic photovoltaic devices.[6] We therefore trust that our results are of relevance for an improved microscopic understanding of such devices. Our results also suggest that time-resolved studies of single QDs shall give distinct and direct information on the tunneling dynamics in such hybrid systems.

The authors acknowledge the financial support by the U.S. NSF via Grant No. DMR-0520550, by the DFG via SPP 1931 and by KICOS (GRL program).

*ymazur@uark.edu
†On leave from Instituto de Física de São Carlos, USP, São Carlos 13560-970, SP, Brazil.

[1] R. W. Schoenlein, L. A. Peteanu, R. A. Mathies, and C. V. Shank, Science **254**, 412 (1991).
[2] T. Pullerits and V. Sundstrom, Acc. Chem. Res. **29**, 381 (1996).
[3] F. Eickemeyer, K. Reimann, M. Woerner, T. Elsaesser, S. Barbieri, C. Sirtori, G. Strasser, T. Muller, R. Bratschitsch, and K. Unterrainer, Phys. Rev. Lett. **89**, 047402 (2002).
[4] C. J. Brabec, N. S. Sariciftci, and J. C. Hummelen, Adv. Funct. Mater. **11**, 15 (2001).
[5] Y. Tachibana, J. E. Moser, M. Gratzel, D. R. Klug, and J. R. Durrant, J. Phys. Chem. **100**, 20056 (1996).
[6] C. J. Brabec, G. Zerza, G. Cerullo, S. De Silvestri, S. Luzzati, J. C. Hummelen, and S. Sariciftci, Chem. Phys. Lett. **340**, 232 (2001).
[7] E. A. Stinaff, M. Scheibner, A. S. Bracker, I. V. Ponomarev, V. L. Korenev, M. E. Ware, M. F. Doty, T. L. Reinecke, and D. Gammon, Science **311**, 636 (2006).
[8] H. J. Krenner, M. Sabathil, E. C. Clark, A. Kress, D. Schuh, M. Bichler, G. Abstreiter, and J. J. Finley, Phys. Rev. Lett. **94**, 057402 (2005).
[9] P. Bhattacharya, S. Ghosh, S. Pradhan, J. Singh, Z.-K. Wu, J. Urayama, K. Kim, and T. B. Norris, IEEE J. Quantum Electron. **39**, 952 (2003).
[10] Z. Mi, P. Bhattacharya, and S. Fathpour, Appl. Phys. Lett. **86**, 153109 (2005).
[11] J. Faist, F. Capasso, C. Sirtori, D. L. Sivco, A. L. Hutchinson, and A. Y. Cho, Nature (London) **387**, 777 (1997).
[12] S. Bar-Ad, P. Kner, M. V. Marquezini, S. Mukamel, and D. S. Chemla, Phys. Rev. Lett. **78**, 1363 (1997).
[13] M. Kroner, A. O. Govorov, S. Remi, B. Biedermann, S. Seidl, A. Badolato, P. M. Petroff, W. Zhang, R. Barbour, B. D. Gerardot, R. J. Warburton, and K. Karrai, Nature (London) **451**, 311 (2008).
[14] P. A. Dalgarno, M. Ediger, B. D. Gerardot, J. M. Smith, S. Seidl, M. Kroner, K. Karrai, P. M. Petroff, A. O. Govorov, and R. J. Warburton, Phys. Rev. Lett. **100**, 176801 (2008).
[15] U. Fano, Phys. Rev. **124**, 1866 (1961).
[16] T. Kakitani, A. Kimura, and H. Sumi, J. Phys. Chem. B **103**,

3720 (1999).
[17] T. F. Boggess, L. Zhang, D. G. Deppe, D. L. Huffaker, and C. Cao, Appl. Phys. Lett. **78**, 276 (2001); E. W. Bogaart, R. Nötzel, Q. Gong, J. E. M. Haverkort, and J. Wolter, *ibid.* **86**, 173109 (2005).
[18] K. W. Sun, A. Kechiantz, B. C. Lee, and C. P. Lee, Appl. Phys. Lett. **88**, 163117 (2006).
[19] O. Verzelen, R. Ferreira, and G. Bastard, Phys. Rev. Lett. **88**, 146803 (2002).
[20] V. G. Talalaev, J. W. Tomm, N. D. Zakharov, P. Werner, U. Gösele, B. V. Novikov, A. S. Sokolov, Y. B. Samsonenko, V. A. Egorov, and G. E. Cirlin, Appl. Phys. Lett. **93**, 031105 (2008).
[21] H. Wang, K. Ferrio, D. G. Steel, Y. Z. Hu, R. Binder, and S. W. Koch, Phys. Rev. Lett. **71**, 1261 (1993).
[22] J. M. Shacklette and S. T. Cundiff, Phys. Rev. B **66**, 045309 (2002).
[23] T. Guenther, C. Lienau, T. Elsaesser, M. Glanemann, V. M. Axt, T. Kuhn, S. Eshlaghi, and A. D. Wieck, Phys. Rev. Lett. **89**, 057401 (2002).
[24] J. Feldmann, G. Peter, E. O. Göbel, P. Dawson, K. Moore, C. Foxon, and R. J. Elliott, Phys. Rev. Lett. **59**, 2337 (1987).
[25] S. L. Chuang and N. Holonyak, Jr., Appl. Phys. Lett. **80**, 1270 (2002).
[26] S.-W. Chang, S.-L. Chuang, and N. Holonyak, Jr., Phys. Rev. B **70**, 125312 (2004).
[27] R. A. Kaindl, M. A. Carnahan, D. Hägele, R. Lövenich, and D. S. Chemla, Nature (London) **423**, 734 (2003).